Research Article

Received: 7 November 2009 Revised: 21 January 2010 Accepted: 8 February 2010 Published online in Wiley Interscience: 29 March 2010

(www.interscience.wiley.com) DOI 10.1002/jctb.2382

Optimization of the process parameters for the removal of boron from drinking water by electrocoagulation – a clean technology

Subramanyan Vasudevan,[a]* Sagayaraj Margrat Sheela,[b] Jothinathan Lakshmi[a] and Ganapathy Sozhan[a]

Abstract

BACKGROUND: There are a number of articles related to removal of boron by electrocoagulation using aluminium electrodes, but there are fewer articles describing the use of magnesium as the anode material. The main disadvantage of aluminium electrodes is the residual aluminium present in the treated water due to cathodic dissolution, which can create health problems. In the case of magnesium electrodes, there is no such disadvantage. This paper presents the results of studies on the removal of boron using magnesium and stainless steel as anode and cathode, respectively.

RESULTS: Results show that a maximum removal efficiency of 86.32% was achieved at a current density of 0.2 A dm^{-2} and pH of 7 using magnesium as the anode and stainless steel as the cathode. The adsorption of boron fitted the Langmuir adsorption isotherm, suggesting monolayer coverage of adsorbed molecules. The adsorption process follows second-order kinetics. Temperature studies showed that adsorption was endothermic and spontaneous in nature.

CONCLUSIONS: The magnesium hydroxide generated in the cell remove the boron present in the water and reduced to a permissible level and making it drinkable. The process scale up results was consistent with the results obtained from the laboratory scale, showing the robustness of the process.

Keywords: boron removal; electrocoagulation; adsorption kinetics; isotherms

INTRODUCTION

Recently boron has come to the forefront as a possible drinking water contaminant. Boron is widely distributed in the environment as calcium and/or sodium borates, such as Colemanite, Ulexite, Tincal, etc., or as a result of anthropogenic pollution mainly in the form of boric acid or borate salts. Boric acid and borate both exist as monomers in solution at low concentration (below 25 mmol L^{-1}), but at higher concentration they appear as highly water soluble poly-borate ions.[1–5] Salts of boron and boric acids are mainly used in the manufacture of glass and porcelain, carpets, cosmetics, in food preservatives, medicines and insecticides and as a neutron absorber in nuclear plants. Since the use and production of boron compounds is huge, surface and groundwater as well as sewage water contains elevated levels of boron.[6–10] In consideration of the toxic effect of boron on humans, the EU and USEPA regulations suggest a guideline of 1.0 mg L^{-1}.[11,12] In humans, signs of boron toxicity include nausea, vomiting, diarrhoea, dermatitis, decreased sexual activity, headache, skin rashes and central nervous system stimulation. The toxicity of its compounds creates a pressing need for investigations aimed at developing effective methods to remove it from aqueous solutions. Removing boron from water is difficult and can be prohibitively expensive and impractical.[9,13,14] Conventional methods for removing boron include coagulation–precipitation, biological processes, ion exchange, membrane technology and electrodialysis.[15–19] In general, conventional processes have disadvantages including incomplete metal removal, they require expensive equipment and monitoring systems, have high reagent and energy requirements or generate toxic sludge or other waste products that require disposal.[17,20]

During the last few decades, electrocoagulation has undergone rapid growth and development. In this process, electrochemically generated metallic ions undergo hydrolysis near the anode to produce a series of activated intermediates that are able to destabilize the finely dispersed particles in the water and wastewater being treated. The advantages of electrocoagulation include high particulate removal efficiency, compact treatment facility, relatively low cost, and the possibility of complete automation.[21–25] Usually magnesium and aluminium plates are used as electrodes for electrocoagulation followed by an electro-sorption process.

* *Correspondence to: Subramanyan Vasudevan, Central Electrochemical Research Institute (CSIR), Karaikudi 630 006, India. E-mail: vasudevan65@gmail.com*

a *Central Electrochemical Research Institute (CSIR), Karaikudi 630 006, India*

b *St Joseph College, Trichy, India*

(i) When magnesium is used as the electrode, the reactions are as follows:

$$\text{At the cathode :} \quad 2H_2O + 2e^- \Rightarrow H_2(g) + 2OH^- \tag{1}$$

$$\text{At the anode :} \quad Mg \Rightarrow Mg^{2+} + 2e^- \tag{2}$$

$$\text{In solution :} \quad Mg^{2+}(aq) + 2H_2O \Rightarrow Mg(OH)_2 \downarrow + 2H^+(aq) \tag{3}$$

(ii) When aluminium is used as electrode, the reactions are as follows:

$$\text{At the cathode :} \quad 2H_2O + 2e^- \Rightarrow H_2(g) + 2OH^- \tag{4}$$

$$\text{At the anode :} \quad Al \Rightarrow Al^{3+} + 3e^- \tag{5}$$

$$\text{In solution :} \quad Al^{3+}(aq) + 3H_2O \Rightarrow Al(OH)_3 \downarrow + 3H^+(aq) \tag{6}$$

Although there are numerous reports related to removal of boron by electrocoagulation using aluminium as the anode,[26–28] reports using magnesium as anode material are scant. The main disadvantage of using aluminium is the presence of residual aluminium in the treated water due to cathodic dissolution. This will create health problems and the USEPA guidelines suggest a maximum contamination of 0.05–0.2 mg L^{-1}. In the case of magnesium electrodes, there is no such disadvantage as the USEPA guidelines suggest a maximum value of magnesium in water of 30 mg L^{-1}.

This work presents the results of the laboratory scale and scale-up studies on the removal of boron using magnesium and stainless steel as anode and cathode, respectively. To optimize the maximum removal efficiency of boron, the effect of current density, initial boron concentration, temperature, pH and effect of co-existing ions like carbonate, phosphate, silicate and arsenic were studied. The adsorption kinetics of electrocoagulants is analyzed using first- and second-order kinetic models. The Langmuir, Freundlich and Dubinin-Radushkevich equilibrium adsorption models were also studied and the activation energy calculated to study the nature of the adsorption.

MATERIALS AND METHODS

Experimental procedure

Figure 1 shows the electrolytic cell consisting of a 1.0 L Plexiglas vessel fitted with a polycarbonate cell cover with slots to introduce the anode, cathode, pH sensor, thermometer and electrolytes. A magnesium sheet (Alfa, UK), 0.14 m × 0.15 m × 0.001 m, surface area 0.02 m^2 acted as the anode and stainless steel (commercial grade, India) sheets of the same size were placed at an inter-electrode distance of 0.005 m. The temperature of the electrolyte was controlled to a variation of ±2 K by adjusting the flow rate of thermostatically controlled water through an external glass cooling spiral. A regulated direct current (DC) was supplied from a rectifier (50 A, 0–25 V; Aplab model, India, L 3230).

Boron as boric acid (H_3BO_4) (Analar Reagent, Merck, Germany) was dissolved in distilled water to the required concentration (3–7 mg L^{-1}). This solution (0.90 L) was used for each experiment as the electrolyte. The pH of the electrolyte was adjusted, if required, with 1 mol L^{-1} HCl or 1 mol L^{-1} NaOH solutions before the start of the experiments. To examine the effect of co-existing ions on the removal of boron, Analar grade sodium salts of carbonate, phosphate, silicate and arsenate were added to the electrolyte at the appropriate concentrations.

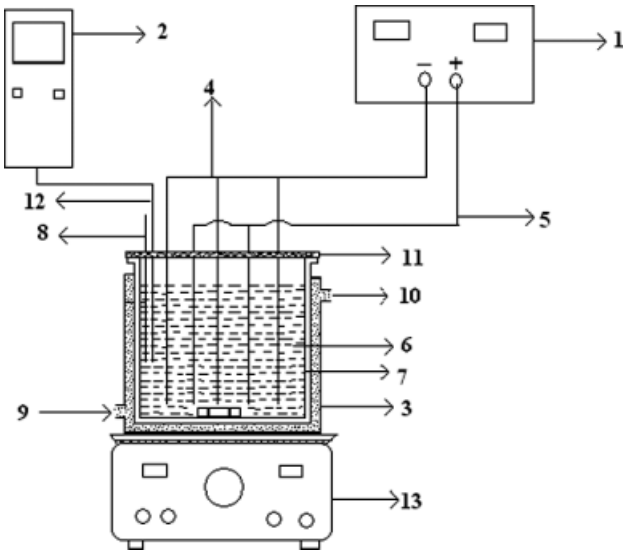

Figure 1. (1) DC power supply, (2) pH meter, (3) electrochemical cell, (4) cathodes, (5) anode, (6) electrolyte, (7) outer jacket, (8) thermostat, (9) inlet for thermostatic water, (10) outlet for thermostatic water, (11) PVC cover, (12) pH sensor, (13) magnetic stirrer.

Analysis

The concentration of boron was determined spectrophotometrically using standard boron kits (Merck, Germany) by UV-visible spectrophotometer (Merck, Pharo 300). The magnesium hydroxide was analyzed with a scanning electron microscope (SEM) (Hitachi model s-3000h, Japan). The Fourier transform infrared spectrum of magnesium hydroxide was obtained using a Nexus 670 FTIR spectrometer (Thermo Electron Corporation, USA) and X-ray diffraction(XRD) patterns of electrocoagulation by-products were analyzed using an X'per PRO X-ray diffractometer (PANalytical, USA).

RESULTS AND DISCUSSION

The effect of amount of coagulant

The current density determines dosage rate of the coagulant in the electrocoagulation process and thus, the current density should have a major impact on pollution removal efficiencies. The amount of boron removed and its removal rate increased with increasing current density. Furthermore, the amount of boron removed depends upon the quantity of adsorbent (magnesium hydroxide) generated, which is related to the time and current density.[29] The amount of adsorbent produced was determined using the Faraday law:[29]

$$E_c = ItM/ZF \tag{7}$$

where I = current (A), t = time (s), M = molecular weight, Z = number of electrons involved, and F = the Faraday constant (96 485.3 coulomb $mole^{-1}$). To investigate the effect

of current density on boron removal, a series of experiments were carried out using solutions containing a constant pollutant loading of 5 mg L^{-1}, with the current density being varied from 0.1–0.5 A dm^{-2}. The removal efficiency was 74.1, 86.3, 89.9, 92.3 and 97.3% for current densities of 0.1, 0.2, 0.3, 0.4 and 0.5 A dm^{-2}, respectively, showing that boron adsorption increases with increase in adsorbent concentration, indicating that the adsorption depends on availability of binding sites for boron.

The effect of pH

The initial pH is one of the important factors affecting the performance of the electrochemical process. To study this effect, a series of experiments were carried out using solutions containing 5 mg L^{-1} boron, with an initial pH in the range 2–10. It was found that boron removal efficiency increased for pH up to 7.0 and then decreased. The maximum removal efficiency of boron at pH 7 was 86.3% and the minimum efficiency was 72% at pH 10. The decrease of removal efficiency with aluminium electrodes at more acidic and alkaline pH values has been observed by many investigators,[17] and is attributed to the amphoteric behaviour of $Al(OH)_3$, leading to soluble Al^{3+} cations (at acidic pH) and monomeric anions $Al(OH)^{4-}$ (at alkaline pH). It is well known that these soluble species are not useful for water treatment. When the initial pH was neutral, all the aluminium produced at the anode formed polymeric species ($Al_{13}O_4(OH)_{24}{}^{7+}$) and precipitated $Al(OH)_3$ leading to greater removal efficiency. In the present study, the electrolyte pH was maintained at neutral, so the formation of $Mg(OH)_2$ predominates leading to greater removal efficiency. Also, when the solution is alkaline, borate ions in solution are predominantly present as $B(OH)_4{}^-$ whereas in acidic solution the borate ions are present as $B(OH)_3$. Thus the highest boron removal efficiency was obtained at pH 7.0 because boron was present as $B(OH)_3$ and the formation of $Mg(OH)_2$ was high.

The effect of initial boron concentration

To study the effect of initial boron concentration, experiments were conducted at varying initial concentrations ranging from 3–7 mg L^{-1}. The adsorption of boron increased with increasing boron concentration and remained constant after equilibrium (Fig. 2), which was reached after 30 min for all concentrations studied. The amount of boron adsorbed (q_e) increased from 1.7914–5.313 mg g^{-1} as concentration increased from 3–7 mg L^{-1}. Figure 2 also shows that in the initial stages, adsorption is rapid and then gradually decreases with progress of adsorption. The plots are smooth and continuous, leading to saturation, suggesting possible monolayer coverage of boron on the surface of the adsorbent.[30]

Effect of coexisting anions

Carbonate

Effect of carbonate on boron removal was evaluated by increasing carbonate concentration in the electrolyte from 5–250 mg L^{-1}. The removal efficiencies are 86.3, 83.2, 51.2, 45.8, 28.1, and 12.3% for the carbonate ion concentration of 0, 2, 5, 65, 150 and 250 mg L^{-1}, respectively. The results show that below 2 mg L^{-1} the removal efficiency of boron is not affected by the presence of carbonate. However, significant reduction in removal efficiency was observed above 5 mg L^{-1} carbonate due to passivation of the anode, reducing dissolution of the anode.

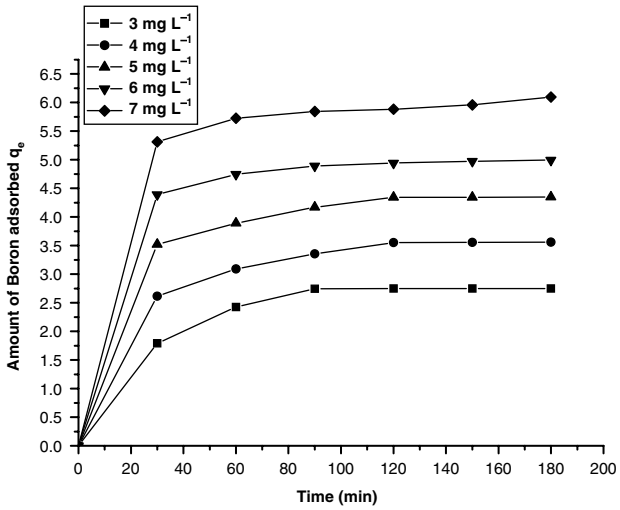

Figure 2. Effect of agitation time and amount of boron adsorbed. Conditions, current density: 0.2 A dm^{-2}; pH of the electrolyte: 7.0; temperature: 305 K.

Phosphate

The concentration of phosphate ion was increased from 2–50 mg L^{-1}, i.e. the range of phosphate in groundwater. The removal efficiency of boron was 86.3, 85.2, 54.4, 48.7 and 40.2% for 0, 2, 5, 25 and 50 mg L^{-1} of phosphate ion, respectively. There was no change in removal efficiency of boron below 2 mg L^{-1} phosphate but at higher concentrations (5 mg L^{-1} and above) the removal efficiency decreased drastically. This is due to the preferential adsorption of phosphate over boron as the phosphate concentration increases.

Arsenic

From the results it is found that the efficiency decreased from 86.3–35.2% on increasing the arsenate concentration from 0.2–5 mg L^{-1}. Like the effect of phosphate, this is due to the preferential adsorption of arsenic over boron as the arsenate concentration increases. Thus, when arsenic is present in the water this strongly competes with boron for the binding sites.

Silicate

The results show no significant change in boron removal when the silicate concentration was increased from 0–2 mg L^{-1}. The respective efficiencies for 0, 2, 5, 10 and 15 mg L^{-1} silicate were 86.3, 84.2, 72.1, 62.4 and 43.1% showing that boron removal decreased with increasing silicate concentration from 2–15 mg L^{-1}. In addition to preferential adsorption, silicate can also interact with magnesium hydroxide to form soluble and highly dispersed colloids that are not removed by normal filtration.

Studies on adsorption kinetics

The variation of the adsorbed boron with time was characterized using first-order and second-order rate equations proposed by Lagergren. The first-order Lagergren model is[31]

$$dq/dt = k_1 (q_e - q_t) \quad (8)$$

where q_t is the amount of boron adsorbed on the adsorbent at time t (min) and k_1 (min^{-1}) is the rate constant for first order

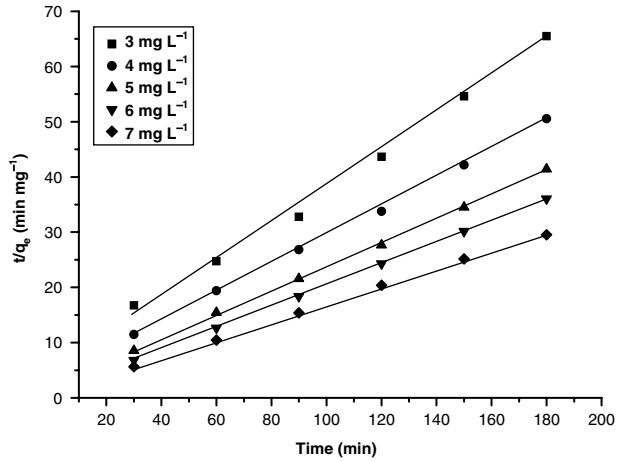

Figure 3. Second-order kinetic model plot for different concentrations of boron. Conditions, current density: 0.2 A dm^{-2}; temperature: 305 K; pH of the electrolyte: 7.

adsorption. The integrated form of the above equation with the boundary conditions $t = 0$ to >0 ($q = 0$ to >0) rearranges to give the following time dependence function:

$$\log (q_e - q_t) = \log (q_e) - k_1 t/2.303 \quad (9)$$

where q_e is the amount of boron adsorbed at equilibrium. The values of q_e and the rate constant (k_1) were calculated from the slope of the plots of log ($q_e - q_t$) versus time (t). It was found that the calculated q_e values did not agree with the experimental values indicating that first-order kinetics were not followed.

The second-order kinetic model is expressed as[32]

$$dq/dt = k_2 (q_e - q_t)^2 \quad (10)$$

where k_2 is the rate constant of second-order adsorption. Integration of equation (10) gives:

$$1/(q_e - q_t) = 1/q_e + k_2 t \quad (11)$$

which can be rearranged and linearized to give:

$$t/q_e = 1/k_2 q_e^2 + t/q_e \quad (12)$$

The second-order kinetic values of q_e and k_2 were calculated from the slope and intercept of the plots t/q_e versus t (Fig. 3). Table 1 gives the computed results from first- and second-order kinetic models. For the second-order kinetics model the calculated and experimental q_e values agree better than those of the first-order kinetic model, indicating that adsorption follows more closely the second-order kinetic model.

Studies on adsorption isotherm

To quantify adsorption capacity of adsorbent the Freundlich, Langmuir and Dubinin–Radushkevich (D-R) isotherm models were analyzed. To determine the isotherms, the initial pH was kept at 7 and the concentration of boron varied over the range 3–7 mg L^{-1}. The Freundlich isotherm is derived to model multilayer adsorption and the empirical isotherm is defined as follows[33]

$$q_e = KC^n \quad (13)$$

According to this model the initial amount of adsorbed compound increases rapidly, then slows down with increasing surface coverage. Equation (13) can be linearised and the Freundlich constants determined as follows[34]

$$\log q_e = \log k_f + n \log C_e \quad (14)$$

where k_f is the Freundlich constant related to adsorption capacity, n is the energy or intensity of adsorption, C_e is the equilibrium concentration of boron (mg L^{-1}). The adsorption data is plotted as log q_e versus log C_e and should result in a straight line with slope n and intercept k_f, indicating adsorption capacity and adsorption intensity. In this study the k_f and n values were 0.4722 (mg g^{-1}) and 0.7804 (L mg^{-1}), respectively. It has been reported that values of n lying between 0 and 10 indicate favourable adsorption. From analysis of the results it is found that Freundlich plots fit satisfactorily with the experimental data. This agrees with published results for adsorption of chromium and arsenic.[30,35]

An alternative equation derived by Langmuir was developed assuming that a fixed number of accessible sites are available on the adsorbent surface, all of which have the same energy; adsorption is reversible; monolayer adsorption occurs and there are no lateral interactions between the adsorbates. Maximum adsorption occurs when molecules adsorbed on the surface of the adsorbent form a saturated layer. The linearized form of the Langmuir adsorption isotherm model is[36]

$$C_e/q_e = 1/q_m k_a + C_e/q_m \quad (15)$$

where C_e is the concentration of the boron solution (mg L^{-1}) at equilibrium, q_m the adsorption capacity (Langmuir constant) and k_a the energy of adsorption. Figure 4 shows Langmuir plots of the experimental data, showing a better fit than for the Freundlich

Table 1. Comparison between experimental and calculated q_e values for different initial boron concentrations in first-order and second-order adsorption isotherm

		First-order adsorption			Second-order adsorption		
Concentration (mg L^{-1})	q_e (expt)	q_e (calc)	$K_1 \times 10^4$ (min mg^{-1})	R^2	q_e (calc)	$K_2 \times 10^4$ (min mg^{-1})	R^2
3	1.7914	30.52	−0.0033	0.7070	2.2711	0.0427	0.9906
4	2.6159	33.01	−0.0057	0.8471	2.9791	0.0377	0.9948
5	3.5198	30.24	−0.0067	0.8307	3.8271	0.0454	0.9974
6	4.3916	30.21	−0.0069	0.9172	4.6521	0.0779	0.9941
7	5.3130	30.18	−0.0074	0.8929	5.5497	0.0544	0.9989

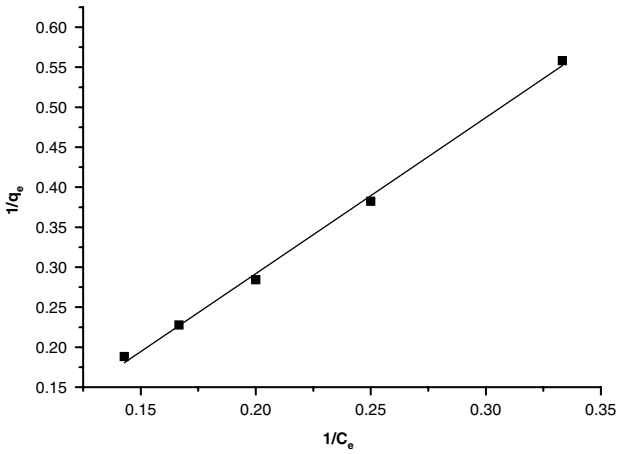

Figure 4. Langmuir plot ($1/C_e$ versus $1/q_e$).

plots. The value of the adsorption capacity (q_m) is 66.67 mg g^{-1}, which is higher than that of other adsorbents studied.

The essential characteristics of the Langmuir isotherm can be expressed as the dimensionless constant R_L[37]

$$R_L = 1/(1 + BC_o) \tag{16}$$

where R_L is the equilibrium constant indicating the type of adsorption, b = the Langmuir constant and C_o = concentration of boron solution. R_L values between 0 and 1 indicate favourable adsorption. In this study R_L values between 0 and 1 were found for all boron concentrations. The results are presented in Table 2.

The Dubinin–Radushkevich isotherm assumes that a characteristic sorption curve is related to the porous structure of the sorbent and apparent energy of adsorption. This model is given by[38]

$$q_e = q_s \exp(-B\varepsilon^2) \tag{17}$$

where ε = Polanyi potential ($= RT \ln(1 + 1/C_e)$, B is related to the free energy of sorption and q_s is the Dubinin–Radushkevich (D-R) isotherm constant.[38] The linearized form is

$$\ln q_e = \ln\ q_s - 2B\,RT \ln[1 + 1/C_e] \tag{18}$$

The isotherm constants q_s and B are obtained from the intercept and slope of the plot of ln q_e versus ε^2.[39] The constant B gives the mean free energy of adsorption per molecule of the adsorbate when it is transferred from the solid from infinity in the solution and the relation is given as

$$E = [1/\sqrt{2B}] \tag{19}$$

The magnitude of E is useful for estimating the type of adsorption process. In this system it was 0.6360 kJ mol^{-1}, which is much smaller than the energy range of physical adsorption reaction[40] (8–16 kJ mol^{-1}) indicating that the adsorption of boron on magnesium was chemical adsorption.

The correlation coefficient values of different isotherm models are listed in Table 2. The Langmuir isotherm model has higher regression co-efficient (R^2 = 0.999) and the value of R_L for the Langmuir isotherm was between 0 and 1, indicating favourable adsorption of boron.

Studies on effect of temperature

To understand the effect of temperature on adsorption, thermodynamic parameters were determined at various temperatures. The amount of boron adsorbed increased with increasing temperature indicating the process was endothermic. The diffusion coefficient (D) for intraparticle transport of boron species into the adsorbent particles can be calculated at different temperatures by[41]

$$t_{1/2} = 0.03x{r_o}^2/D \tag{20}$$

where $t_{1/2}$ = time of half adsorption (s), r_o = the radius of the adsorbent particle (cm), D = the diffusion coefficient ($cm^2\ s^{-1}$). For all chemisorption systems the diffusivity coefficient should be between 10^{-5} and 10^{-13} $cm^2\ s^{-1}$.[41] In the present work, D was found to be in the region of 10^{-10} $cm^2\ s^{-1}$. The pore diffusion coefficient (D) values for various temperatures and different initial concentrations of boron are presented in Table 3. To find the energy of activation for boron adsorption the second-order rate constant is expressed in Arrhenius form[30]

$$\ln k_2 = \ln k_o - E/RT \tag{21}$$

where k_o = the constant of the equation (g mg^{-1} min^{-1}), E = the energy of activation (J mol^{-1}), R = the gas constant (8.314 J mol^{-1} K^{-1}) and T = the temperature (K). Figure 5 shows that the rate constants vary with temperature according to Equation (21) giving an activation energy of 0.396 kJ mol^{-1} from the slope of the fitted equation. The free energy change can be obtained as[30]

$$\Delta G = -RT \ln K_c \tag{22}$$

where ΔG = the free energy (kJ mol^{-1}), K_c = the equilibrium constant, R = the gas constant and T = temperature (K). The values of K_c and ΔG are presented in Table 4. The negative value of ΔG indicates the spontaneous nature of adsorption. Other thermodynamic parameters such as entropy change (ΔS) and enthalpy change (ΔH) were determined using the van't Hoff equation:

$$lnK_c = \frac{\Delta S}{R} - \frac{\Delta H}{RT} \tag{23}$$

Table 2. Constant parameters and correlation coefficient for different adsorption isotherm models for boron adsorption at 5 mg L^{-1}

Isotherm	Constants			
Langmuir	Q_0 (mg g^{-1})	b (L mg^{-1})	R_L	R^2
	66.67	0.0021	0.9053	0.9997
Freundlich	K_f (mg g^{-1})	n (L mg^{-1})		R^2
	0.4722	0.7804		0.9986
D-R	Q_s ($\times 10^3$ mol g^{-1})	B ($\times 10^3$ mol^2 kJ^{-2})	E (kJ mol^{-1})	R^2
	0.397	0.458	0.6307	0.8994

Table 3. Pore diffusion coefficients for the adsorption of boron at different concentrations at 305 K and at different temperatures between 313 and 343 K at 5 mg L^{-1}

Concentration (mg L^{-1})	Pore diffusion constant $D \times 10^{-9}$ (cm^2 s^{-1})
3	2.35
4	1.18
5	0.78
6	0.47
7	0.39
Temperature (K)	**Pore diffusion constant $D \times 10^{-9}$ (cm^2 s^{-1})**
313	0.47
323	0.78
333	1.18
343	2.35

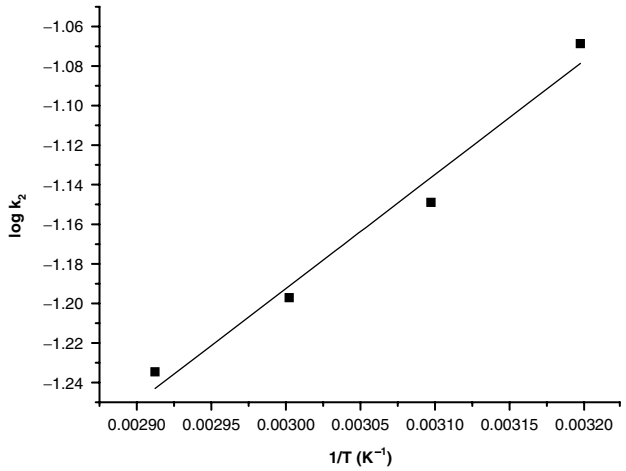

Figure 5. Plot of log k_2 versus $1/T$.

Table 4. Thermodynamic parameters for adsorption of boron

Temperature (K)	K_c	ΔG^o (J mol^{-1})	ΔH^o (kJ mol^{-1})	ΔS^o (J mol^{-1} K^{-1})
313	1.0468	−119.26		
323	1.0888	−228.61	3.416	11.289
333	1.1318	−342.91		
343	1.1738	−457.18		

The enthalpy change ($\Delta H = 3.416$ J mol^{-1}) and entropy change ($\Delta S = 11.289$ J mol^{-1} K^{-1}) were obtained from the slope and intercept of the van't Hoff plots of lnK_c versus $1/T$ (Fig. 6). Positive values of enthalpy change (ΔH) indicate an endothermic adsorption process and negative values of change in internal energy (ΔG) show spontaneous adsorption of boron. Positive values of entropy change show the increased randomness of the solution interface during boron adsorption (Table 4). Enhancement of the adsorption capacity of the magnesium hydroxide electrocoagulant at higher temperatures may be attributed to enlargement of pores and/or activation of the adsorbent surface. Using the Lagergren rate equation, first-order rate constants and correlation co-efficient were calculated for different temperatures (305–343 K). The

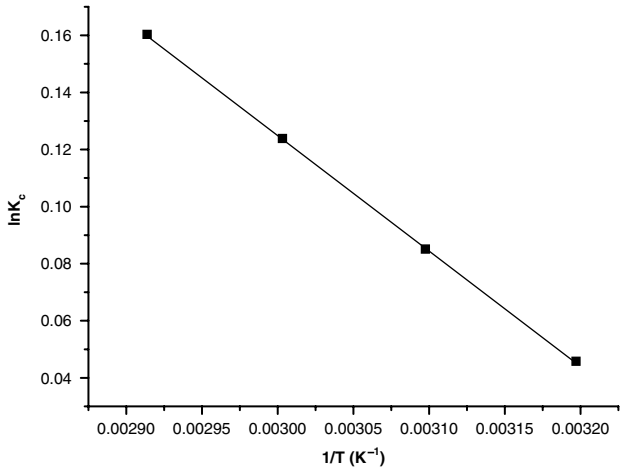

Figure 6. Plot of ln K_c versus $1/T$.

calculated q_e values obtained from the second-order kinetics agree with the experimental q_e values better than those from the first-order kinetics model. Table 5 depicts the computed results obtained from first- and second-order kinetic models, indicating that adsorption follows second-order kinetics over the temperatures used in this study.

PROCESS SCALE-UP

On the basis of results obtained at laboratory scale, a large capacity cell was designed, fabricated and operated to remove boron from drinking water. A cell [(0.35 m (l) × 0.25 m (w) × 0.25 m (h)] was fitted with PVC cover with holes to introduce the anode, cathode, thermometer and electrolyte. A magnesium anode (0.17 m (w) × 0.18 m (h) × 0.001 m (t)) was used and the cathode was a stainless steel plate of the same dimensions. The cell was operated at 0.2 A dm^{-2} and contained electrolyte (8.5 L) at a pH of 7.0. Results showed that a maximum removal efficiency of 86.1% was achieved at a current density of 0.2 A dm^{-2} at pH = 7. The results were consistent with the results obtained at laboratory scale, showing the robustness of the process.

SEM, XRD and FTIR analysis

SEM studies

Figure 7 shows an SEM image of the magnesium anode after several cycles of use. The electrode surface is rough, with a number of depressions. These are formed around the nucleus of the active sites where electrode dissolution results in the production of magnesium hydroxide. The formation of a large number of depressions may be attributed to anode consumption at active sites due to oxygen generation at its surface.

FTIR studies

Figure 8 shows the FTIR spectrum of boron–magnesium hydroxide. A broad adsorption band at 3448.85 cm^{-1} implies the transformation from free protons into a proton-conductive state in brucite.[42] The 1641.19 cm^{-1} peak indicates the bent vibration of H-O-H. The absorbance at 565.13 cm^{-1} represents the Mg–borate linkage[43] and the band at 665.18 corresponds to Mg–O stretching vibration.[44]

Table 5. Comparison between experimental and calculated q_e values for a boron concentration of 5 mg L^{-1} in first- and second-order adsorption kinetics at different temperatures

		First-order adsorption			Second-order adsorption		
Temp. (K)	q_e (expt)	q_e (calc)	$K_1 \times 10^4$ (min mg^{-1})	R^2	q_e (calc)	$K_2 \times 10^4$ (min mg^{-1})	R^2
313	3.6257	30.24	−0.0024	0.7965	3.6737	0.0854	0.9979
323	3.7392	33.71	−0.0057	0.7100	3.9860	0.0709	0.9977
333	3.8182	34.58	−0.0075	0.8167	4.1561	0.0635	0.9976
343	3.9936	34.80	−0.0071	0.8683	4.2936	0.0583	0.9983

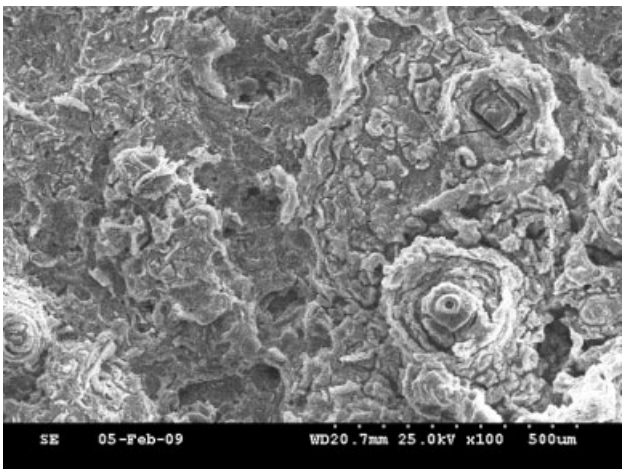

Figure 7. SEM images of magnesium anode after electrocoagulation of boron electrolyte.

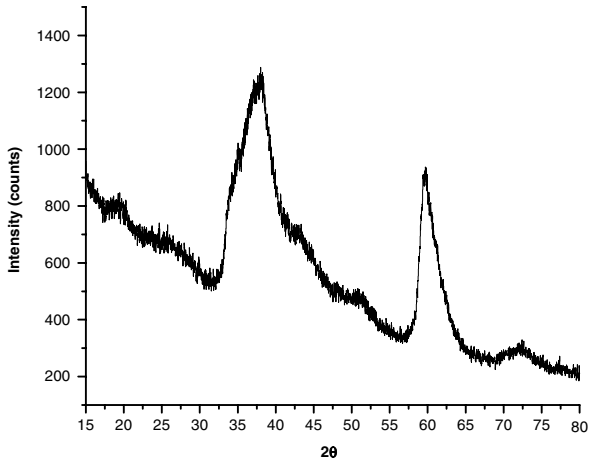

Figure 9. XRD spectra of Mg–Boron electrocoagulant.

XRD studies

An X-ray diffraction spectrum of the magnesium electrode coagulant showed very broad and shallow diffraction peaks (Fig. 9). These broad humps and low intensity indicate the coagulant is amorphous or very poorly crystalline in nature. This may be due to the crystallization of magnesium hydroxide being a very slow process so that all the magnesium hydroxides were either amorphous or very poorly crystalline.

CONCLUSION

In this investigation of the removal of boron from drinking water results showed that a maximum removal efficiency of 86.3%

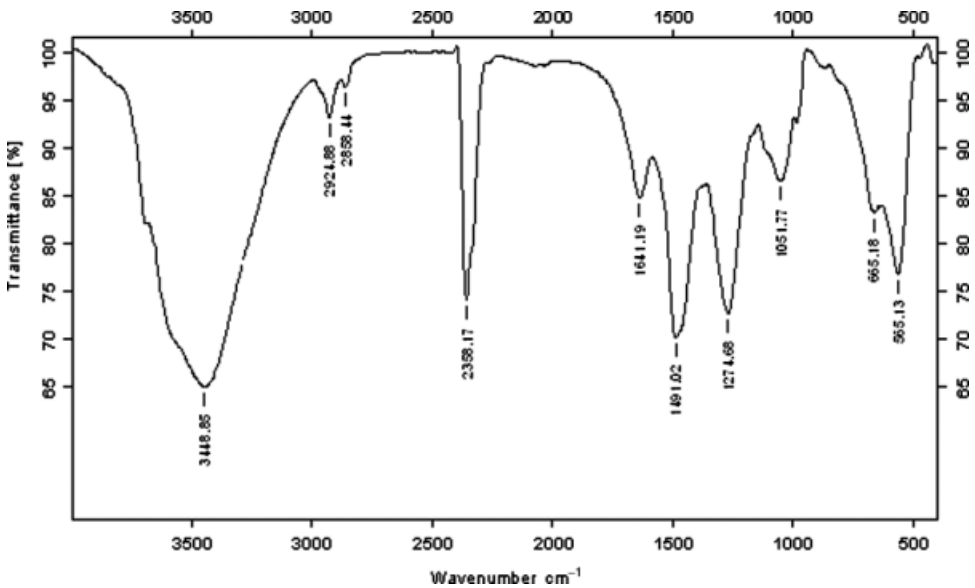

Figure 8. FTIR spectrum of boron-adsorbed magnesium hydroxide.

was achieved by electrocoagulation at a current density of 0.2 A dm^{-2} and a pH of 7 using magnesium as the anode and stainless steel as the cathode. The magnesium hydroxide generated in the cell removes boron in the water, reducing the concentration to acceptable levels and making it drinkable. The adsorption of boron fits the Langmuir adsorption isotherm, suggesting monolayer coverage of adsorbed molecules. The adsorption process follows second-order kinetics. Temperature studies showed that adsorption was endothermic and spontaneous in nature.

ACKNOWLEDGEMENTS

The authors wish to express their gratitude to the Director, Central Electrochemical Research Institute, Karaikudi for permission to publish this paper.

REFERENCES

1 Peter A, Distribution of boron in the environment. *Bio Trace Element Res* **66**:131–143 (1998).
2 Senkal BK and Bicak N, Polymer supported iminodipropylene glycol functions for removal of boron. *React Funct Polym* **55**:27–33 (2003).
3 Kistler RB and Helvaci C, Boron and Borates. *Industrial Minerals and Rocks*, 6th edn, ed by Carr DD. SME Inc., USA, pp. 171–186 (1994).
4 Bryjak M, Wolska J and Kabay N, Removal of boron from seawater by adsorption–membrane hybrid process: implementation and challenges. *Desalinaton* **223**:57–62 (2008).
5 Yurdakoc M, Seki Y, Karahan S and Yurdakoc K, Kinetic and thermodynamic studies of boron removal by Siral 5, Siral 40 and Siral 80. *J Colloid Interface Sci* **286**:431–440 (2005).
6 Baek KW, Song SH, Kang SH, Rhee YW, Lee CS, Lee BJ, *et al*, Adsorption kinetics of boron by anion exchange resin in packed column bed. *J Ind Eng Chem* **13**:452–456 (2007).
7 Sartaj M and Fernandes L, Adsorption of boron from landfill leachate by peat and the effect of environmental factors. *J Environ Eng Sci* **4**:19–28 (2005).
8 Bouguerra W, Mnif A, Hamroouni B and Dhahbi M, Boron removal by adsorption onto activated alumina and by reverse osmosis. *Desalination* **223**:31–37 (2008).
9 Xu Y and Jiang JQ, Technologies for boron removal. *Ind Eng Chem Res* **47**:16–24 (2008).
10 Kabay N, Arar O, Acar F, Ghazal A, Yuksel U and Yuksel M, Removal of boron from water by electrodialysis: effect of feed characteristics and interfering ions. *Desalination* **223**:63–72 (2008).
11 World Health Organisation, *Guidelines for Drinking-Water Quality*, 2nd edn. WHO (1998).
12 Jiang JQ, Xu Y, Quill K, Simon J and Shettle K, Laboratory study of boron removal by Mg/Al double-layered hydroxides. *Ind Eng Chem Res* **46**:4577 (2007).
13 Ennil Kose T and Ozturk N, Boron removal from aqueous solutions by ion-exchange resin: column sorption–elution studies subscription. However, 1. *J Hazard Mater* **152**:744–749 (2008).
14 Bick A and Ora G, Post-treatment design of seawater reverse osmosis plants: boron removal technology selection for potable water production and environmental control. *Desalination* **178**:233–246 (2005).
15 Srivastava VC, Mall ID and Mishra IM, Characterization of mesoporous rice husk ash (RHA) and adsorption kinetics of metal ions from aqueous solution onto RHA. *J Hazard Mater* **B134**:257–267 (2006).
16 Inglezakis VJ, Loizidou MD and Grigoropoulou HP, On exchange of Pb^{2+}, Cu^{2+}, Fe^{3+} and Cr^{3+} on natural clinoptilolite: selectivity determination and influence of acidity on metal uptake. *J Colloid Interf Sci* **261**:49–54 (2003).
17 Sayiner G, Kandemirli F and Dimoglo A, Evaluation of boron removal by electrocoagulation using iron and aluminum electrodes. *Desalination* **230**:205–212 (2008).
18 Vik EA, Carlson DA, Eikum AS and Gjessing ET, Electrocoagulation of potable water. *Water Res* **18**:1355–1360 (1984).
19 Thella K, Verma B, Srivastava CV and Srivastava KK, Electrocoagulation study for the removal of arsenic and chromium from aqueous solution. *J Environ Sci Health Part A* **43**:554 (2008).
20 Sahin S, A mathematical relationship for the explanation of ion exchange for boron adsorption. *Desalination* **143**:35–43 (2003).
21 Jiang JQ, Xu Y, Simon J, Quill K and Shettle K, Integrated chemical–physical processes kinetic modelling of multiple mineral precipitation problems. *Water Sci Technol* **53**:65–73 (2006).
22 Chen X, Chen G and Yue PL, Modeling the electrolysis voltage of electrocoagulation process using aluminum electrodes. *Chem Eng Sci* **57**:2449–2455 (2002).
23 Chen G, Electrochemical technologies in wastewater treatment. *Sep Purif Technol* **38**:11–41 (2004).
24 Adhoum N and Monser L, Decolorization and removal of phenolic compounds from olive mill wastewater by electrocoagulation. *Chem Eng Process* **43**:1281–1287 (2004).
25 Nadav N, Boron removal from seawater reverse osmosis permeate utilizing selective ion exchange resin. *Desalination* **124**:131–135 (1999).
26 Nihal B¸ Salim O, Hilal YA and Anatholy D, Removal of boron by electrocoagulation. *Environ Chem Lett* **2**:51–54 (2004).
27 Yilmaz EA, Boncukcuoglu R, Muhtar Kocakerim M, Tolga Yilmaz M and Paluluoglu C, Boron removal from geothermal waters by electrocoagulation. *J Hazard Mater* **153**:146–151 (2008).
28 Yilmaz EA, Boncukcuoglu R and Muhtar Kocakerim M, An empirical model for parameters affecting energy consumption in boron removal from boron-containing wastewaters by electrocoagulation. *J Hazard Mater* **144**:101–107 (2007).
29 Golder AK, Samantha AN and Ray S, Removal of phosphate from aqueous solutions using calcined metal hydroxides sludge waste generated from electrocoagulation. *Sep Purif Technol* **52**:102–109 (2006).
30 Namasivayam C and Prathap K, Recycling Fe(III)/Cr(III) hydroxide, an industrial solid waste for the removal of phosphate from water. *J Hazard Mater* **123B**:127–134 (2005).
31 Singh KK, Rastogi R and Hasan SH, Removal of cadmium from wastewater using agriculture waste rice polish. *J Hazard Mater* **121A**:51–58 (2005).
32 Mckay G and Ho YS, The sorption of lead(II) ions on peat. *Water Res* **33**:578–584 (1999).
33 Gasser MS, Morad GH and Aly HF, Batch kinetics and thermodynamics of chromium ions removal from waste solutions using synthetic adsorbents. *J Hazard Mater* **142**:118–129 (2007).
34 Uber FH, Die adsorption in losungen. *Z Phy Chem* **57**:387–470 (1906).
35 Namasivayam C and Senthil Kumar S, Removal of Arsenic(V) from aqueous solutions using industrial solid waste: adsorption rates and equilibrium studies. *Ind. Eng. Chem. Res.* **37**:4816–4822 (1998).
36 Langmuir I, The adsorption of gases on plane surfaces of glass, mica and platinum. *J Am Chem Soc* **40**:1361–1403 (1918).
37 Michelson LD, Gideon PG, Pace EG and Kutal LH, US Department of Industry, *Office of Water Research and Technology Bulletin* Washington DC, (1975).
38 Tan IAW, Hameed BH and Ahmed AL, Equilibrium and kinetic studies on basic dye adsorption by oil palm fibre activated carbon. *Chem Eng J* **127**:111–119 (2007).
39 Demiral H, Demiral I, Tumsek F and Karacbacakoglu B, Adsorption of chromium(VI) from aqueous solution by activated carbon derived from olive bagasse and applicability of different adsorption models. *Chem Eng J* **144**:188–196 (2008).
40 Oguz E, Adsorption characteristics and kinetics of the Cr(VI) on the Thuja oriantalis. *Colloid Surf A* **252**:121–128 (2005).
41 Yang XY and Al-Duri B, Application of branched pore diffusion model in the adsorption of reactive dyes on activated carbon. *Chem Eng J* **83**:15–23 (2001).
42 Hernandez-Moreno MJ, Ulibarri MA, Renon JL and Serna CJ, IR characteristics of hydrotalcitelike compounds. *Phys Chem Miner* **12**:34–38 (1985).
43 Weir CE and Lippincott ER, Infrared studies of aragonite. *J.Res.Nat 1.Bur.Standards*, **65A**:173 (1961).
44 Ostermeier M, Limberg C, Herwig C and Ziemer B, Stabilizing the Boat Conformation of Piperazines Coordinated to Iron(II): *iso*-Butyl Substituents Lead to Robust Oxidation Catalysts via Hyperconjugation. *Z Anorg Allg Chem* **635**:1823–1830 (2009).

